JACS JOURNAL OF THE AMERICAN CHEMICAL SOCIETY

COMMUNICATION

pubs.acs.org/JACS

Chiral Transformation: From Single Nanowire to Double Helix

Yong Wang,[†] Qingxiao Wang,[‡] Hang Sun,[†] Weiqing Zhang,[§] Gang Chen,[†] Yawen Wang,[†] Xiaoshuang Shen,[†] Yu Han,[‡] Xianmao Lu,[§] and Hongyu Chen*,[†]

[†]Division of Chemistry and Biological Chemistry, Nanyang Technological University, Singapore 637371

[‡]Advanced Membranes and Porous Materials Center & Core Lab of Imaging and Characterization, King Abdullah University of Science and Technology, Saudi Arabia 23955-6900

[§]Department of Chemical and Biomolecular Engineering, National University of Singapore, Singapore 117576

S Supporting Information

ABSTRACT: We report a new type of water-soluble ultrathin Au−Ag alloy nanowire (NW), which exhibits unprecedented behavior in a colloidal solution. Upon growth of a thin metal (Pd, Pt, or Au) layer, the NW winds around itself to give a metallic double helix. We propose that the winding originates from the chirality within the as-synthesized Au−Ag NWs, which were induced to untwist upon metal deposition.

Chirality is a major theme in organic chemistry, but it has yet to be fully explored in nanoscience. Chiral nano-objects are of great importance for fabricating future nanodevices, as clearly demonstrated by macroscopic chiral components such as gears, springs, propellers, and scissors. The asymmetric organization of the surface atoms or ligands on small (<5 nm) nanoparticles (NPs) is useful for asymmetric catalysis,[1a] chiral separation,[1b] and novel optical properties.[1c−f] Great efforts have been devoted to reducing the high symmetry of NPs. In contrast to the syntheses of Janus (two-sided) NPs,[2] the available synthetic strategies for less symmetric chiral nano-objects are very limited. Most of the chiral nanostructures in the literature were fabricated using chemical vapor deposition (CVD).[3] Because of the high temperature growth on bulk substrates, they were typically large and nonmetallic. In colloids, a popular approach was to use chiral biomolecules or polymers as templates for the surface assembly of NPs.[1c−e] Chiral NWs were also made in confined environments.[4] But intrinsic chiral NWs were extremely rare.[5a,b]

To date, a majority of the reported nanostructures were of single component,[6] but this simplicity limits their structural variety. We are interested in multicomponent systems that offer new synthetic strategies and novel architectures.[4b,c,7] Of particular interest to us is the environment-responsive shape transformation of nanostructures, which is of critical importance for developing smart nanodevices. Previously, we showed that the polymer shells on Au NWs[4b] or carbon nanotubes[4c] could be induced to contract, coiling the embedded nanofilaments into ring structures. It was the first system that can transform the entire population of colloidal nanostructures.

Here, we report a new system where a population of nanostructures undergoes predictable shape transformation. Ultrathin Au−Ag alloy NWs are first fabricated using a new method. Upon growth of an additional metal layer (Pd, Pt, or Au), the NWs wind around themselves to form double helices (93.5% yield for Pd). By systematic analysis of reaction conditions, we show that the rate of metal deposition was a critical factor in inducing the winding of NWs. The winding action probably originates from the chirality within the as-synthesized Au−Ag alloy NWs, which likely have the Boerdijk-Coxeter-Bernal (BCB) type twisted lattice.[5b]

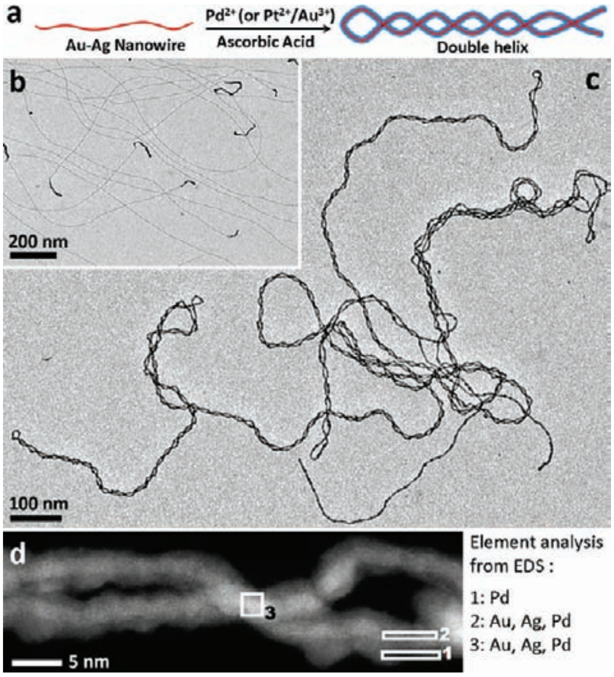

Figure 1. (a) Schematics illustrating the formation of double helix by growing a metal layer on Au−Ag alloy NW; TEM image of (b) the as-synthesized Au−Ag NWs, and (c) a typical (Au−Ag)@Pd double helix; (d) HAADF-STEM image of a typical (Au−Ag)@Pd double helix, showing its core−shell NWs. See the Supporting Information for EDS analyses at the bracketed regions.

The Au−Ag alloy NWs were synthesized by incubating $HAuCl_4$ (final concentration: 0.962 mM), $AgNO_3$ (0.962 mM), ascorbic acid (38.5 mM), and polyvinylpyrrolidone (PVP, 48.1 mM) in a DMF/water mixture (1.04 mL, v/v 7.7:1) at room temperature for 10 days.[8] The product NWs exhibited a brown red color. To purify the NWs, they were precipitated by acetone, washed by water to remove the excess PVP, and finally isolated by centrifugation. From the transmission electron microscopy (TEM) images (Figure 1b),

Received: August 28, 2011
Published: November 17, 2011

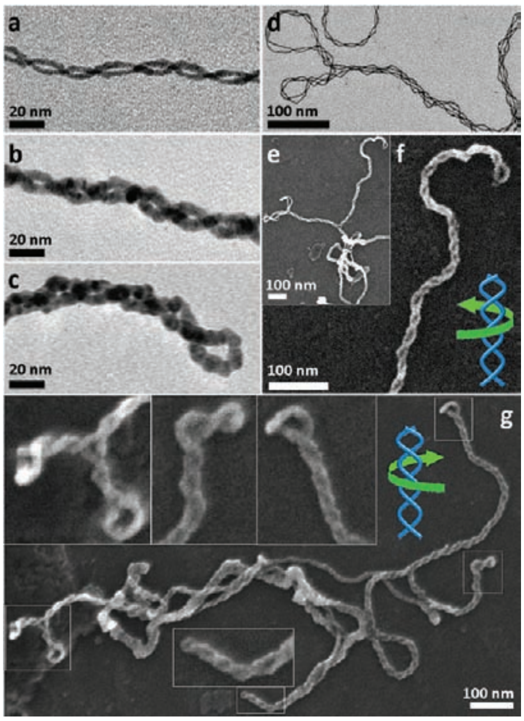

Figure 2. TEM images of (a, b, c) the (Au−Ag)@Pd double helices formed by using ascorbic acid to reduce 80, 270, and 540 μM H_2PdCl_4, respectively; (d) a (Au−Ag)@Pd quadruple helix; and SEM images of (Au−Ag)@Pd double helices of different chirality: (e, f) right-handed; (g) left-handed: in this image, the 4 magnified regions show the same chirality.

the NWs have an averaged diameter of 2 nm and overall length of several micrometers. They often have thicker tails of 4−10 nm in diameter and 70−200 nm in length. Energy dispersive X-ray spectroscopy (EDS) revealed that the central thin section was composed of Au and Ag of about 1:1 in atomic ratio (uniformly distributed[8]), different from the tails (about 4:1). These water-soluble ultrathin NWs were similar in diameter to the hydrophobic ones synthesized in nonpolar solvents using oleylamine as the ligand.[5b,9] In polar solvent, there were only two known cases of ultrathin NWs.[10] Like those in the literature, our ultrathin NWs were easily broken upon heating[4b] or under TEM electron beam.[11]

To our great interest, the alloy NWs formed double helices upon deposition of an additional metal layer at room temperature. The best results occurred with Pd deposition. Briefly, the as-synthesized Au−Ag NWs were added into an aqueous solution of ascorbic acid, followed by Pd precursor (aq H_2PdCl_4). The mixture (DMF/water = 1:13.7, v/v) was gently mixed and then incubated for 1 h without stirring (to rule out the effect of swirling solution). The samples were directly dried on TEM grids without purification,[8] in order to gain accurate survey without losing nanostructures. Figure 1c showed a typical TEM image of the resulting NWs after the Pd growth. The average diameter of the NWs increased to 3.5 nm (Figure 2a), and the NWs tightly wound around themselves to give double helices. They were highly periodic, with uniform pitch length of 47 ± 7 and 2.7 nm gap separating the two intertwined NW sections. Only the helical region near the two ends (one with a U turn and one with two open strands) had irregular and longer pitch periods. To confirm the materials composition in the NWs, we carried out high-angle annular dark-field scanning TEM (HAADF-STEM) and EDS analyses (Figure 1d). Each strand of the double helix consisted of coaxial core−shell (Au−Ag)@Pd NWs, with Pd forming a nonuniform coating.

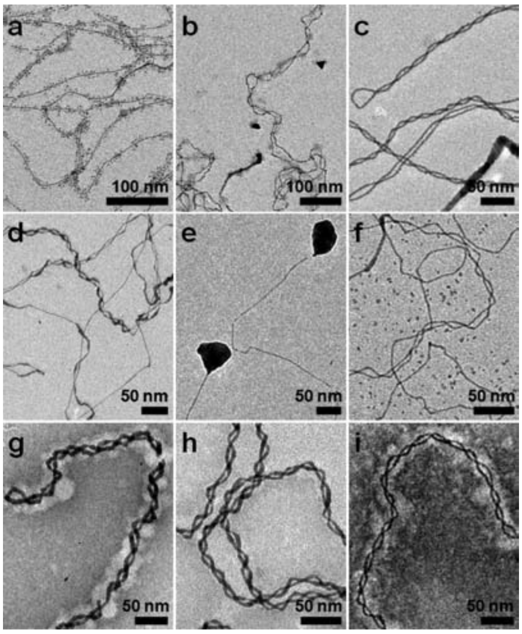

Figure 3. TEM images of the resulting NWs when (a) the purified Au−Ag NWs were incubated with aq H_2PdCl_4 for 24 h; (b) sample a after addition of ascorbic acid, $t = 2$ h (same below); (c) K_2PtCl_4 reacted with ascorbic acid; (d) $HAuCl_4$ with ascorbic acid; (e) $AgNO_3$ with ascorbic acid; (f) H_2PdCl_4 with $NaBH_4$; (g) $HAuCl_4$ with pyrrole; (h) $HAuCl_4$ with aniline; and (i) H_2PdCl_4 with pyrrole.

Survey of the sample showed that most of the NWs transformed to double helices (93.5% out of 246 surveyed). The rest 6.5% of NWs grew thicker without forming any helical region. As judged by the number of open strands (Figure 1c), the NWs did not intertwine with each other, and nearly all helices were derived from the self-winding of individual NWs. Some NWs formed multiple U-turn ends (Figure 2g), and some even formed quadruple helices (Figures 1c, 2d). The latter should result from continued twisting of a double helix. Scanning electron microscopy (SEM) study revealed that both left- and right-handed helices existed in the sample (Figure 2e−g). However, in each helix, the chirality was *always* consistent. The multiple U-turn ends in Figure 2g showed the same winding direction.

Further control experiments established that the NWs did not wind in the absence of H_2PdCl_4, with all other conditions unchanged.[8] On the other hand, without ascorbic acid, the purified Au−Ag NWs reacted with H_2PdCl_4 to give only straight NWs with small Pd NPs attached to their surface (Figure 3a). It was an expected result of the galvanic reaction[12] between H_2PdCl_4 and Ag (the remaining Au/Ag ratio[8] was 1.62). After reacting for 24 h, ascorbic acid was added to the mixture to reduce the remaining Pd^{2+}. The NWs were still able to form helices (Figure 3b), although they were loose with increased pitch period. Hence, the loss of Ag from the Au−Ag NWs seemed to have compromised their ability to wind, and this correlation indicates the critical role of the alloy NWs in forming helices. Another important factor was the Pd deposition on the NWs, as opposed to the Pd−Ag galvanic exchange. As the

H_2PdCl_4 concentration was increased from the original 80 μM to 270 and 540 μM, after its reduction the NWs in the resulting helices increased in thickness to 7 and 10 nm, respectively (Figure 2b,c). The NWs did not fuse together and the pitch length remained the same; only the gap distance between the NWs decreased significantly. Thus, the helix formation was finished after the initial Pd deposition.

Pd was not unique in inducing the helix formation. In the following, we used a same batch of Au−Ag NWs for testing the reaction conditions. When H_2PdCl_4 was replaced by K_2PtCl_4, double helices were also obtained. There were tightly wound helices (Figure 3c) with the same average pitch length and gap separation as those in Figure 2a, but there were also loose helices with kinks that have lost the potential to wind. When $HAuCl_4$ was used as the metal precursor, shortly after the addition of ascorbic acid (<1 min)[8] the color of the solution changed from brown red to the final light purple color, indicating the fast reaction. The yield of double helices was only 10.6% and they have irregular NW width (Figure 3d). Most of the NWs simply grew thicker and formed kinks, and this result was not improved when more $HAuCl_4$ was used. When $AgNO_3$ was used, no helix was formed. The Ag selectively deposited at both ends of the NWs (Figure 3e) with the middle section unchanged.

The above reaction conditions have already been optimized. After careful analysis of numerous initial reactions, we noticed that the yield of helix formation depended critically on the purification step. The residue DMF in the reaction mixture was found to play an important role, probably via affecting the reaction rate. To illustrate this point, the purified Au−Ag NWs were dispersed in either water (0 M DMF) or DMF/water mixture (v/v = 1:13.7, i.e., 0.88 M DMF). After mixing with H_2PdCl_4 and ascorbic acid, the solutions were incubated for 2 h. The rates of Pd reduction were clearly different as indicated by the color change and confirmed by UV−vis kinetics (all reactions were finished within 8 min).[8] The faster reaction in water gave kinked NWs and *loose* double helices (76.6% yield; no improvement after 24 h). In contrast, the presence of the 0.88 M of DMF residue led to slower reaction but higher yield (90.1%) of tightly wound helices. In comparison to the original reaction using the as-synthesized Au−Ag NWs (DMF/water = 1:13.7), these experiments using purified NWs ruled out the effects of PVP and other residue chemicals.

We varied the reactants as an alternative approach to tune the rates of metal reduction in the presence of Au−Ag NWs. When $NaBH_4$ was used as the reductant for H_2PdCl_4, the solution reached the final brown color instantaneously (<1 s). Only a few loose double helices formed and the NWs contained many kinks (Figure 3f).[8] It appeared that the kink formation was correlated with the fast reaction rate, probably because the metal deposition was too fast for the NWs to respond by winding. The additional metal layer might have hardened the NWs and the lattice strain was only relieved in a few spots in the form of kinks. On the other hand, aniline and pyrrole were known to cause slow reduction of $AgNO_3$ or $HAuCl_4$, leading to simultaneous formation of polymer shells.[7a−c] The reduction of $HAuCl_4$ by pyrrole was significantly slower than that using ascorbic acid. After 10 h, this slower reaction gave much improved yield of double helices (from 10.6% to 88.3%). Their structure was also improved in terms of tightly wound helices and uniform NW diameter (Figure 3g). Similarly, the reaction of $HAuCl_4$ with aniline was also slow (10 h), giving 89.8% yield (Figure 3h). The reaction of H_2PdCl_4 with pyrrole did not affect the helix formation; after 10 h, tightly wound double helices were still obtained with good yield (Figure 3i). Control experiments showed that polymer coating without metal deposition cannot induce the helix formation: $(NH_4)_2S_2O_8$ was used to oxidize pyrrole, and the Au−Ag NWs remained straight after the polymer coating.[7d,8]

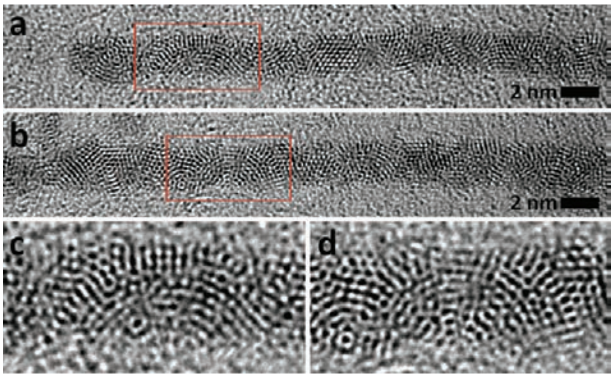

Figure 4. HRTEM images of as-synthesized Au−Ag NWs: (a) a middle section near a broken point; (b) a typical unbroken NW; (c, d) the bracketed regions in a, b, respectively.

With our systematic study in the reaction conditions, the formation of double helices became highly reproducible and the yield improved significantly. Most importantly, the chemistry of the Au−Ag NWs offers mechanistic insights unattainable by physical characterization. The rate of metal deposition was clearly critical: making the Pd reduction faster worsened the yield of double helices, whereas slowing the Au reduction improved the yield. Moreover, the formation of kinked NWs and loose double helices was correlated with the reaction rates as well as the depletion of Ag from the NWs. Control experiments without winding can rule out the effects of external forces. Hence, the NW winding must arise from the *interaction* between the metal coating and the embedded Au−Ag NW. On the other hand, Au and Ag have matching lattices (0.1% mismatch), but Au−Pd (4.71%) and Au−Pt (3.80%) have larger lattice mismatch.[13] The fact that both Pd and Au deposition can cause double helix formation suggests that the lattice matching was probably not a key factor.

The chirality of an individual double helix was remarkably consistent over micrometers in length (Figure 2g). It is impossible for random metal deposition on one end to influence that on the other. Hence, the embedded Au−Ag NW is likely the origin of the chiral action. Following the same logic, random defects in the NW cannot explain the phenomenon: they will most likely cancel out each other in terms of induced action. Given the fast diffusion rate of noble metal atoms, high-density defects are rare in ultrathin NWs.[14] For random polycrystalline NWs, without templates the different parts lack a means to coordinate and achieve uniform width and chirality. Thus, *lattice order* in the Au−Ag NWs is the only conceivable explanation for the uniform NWs and their consistent action.

To study the origin of winding action of the NWs, it is obvious that their central ultrathin section (Au/Ag = 1:1) is more important that their thicker tails. A seminal work published very recently by José-Yacamán and co-workers showed that Au−Ag alloy can form ultrathin NWs (d = 2−5 nm, Au/Ag = 1:3) with BCB type twisted lattice (the twisting was not a result of strain). The authors showed that 2 or more BCB type spirals can be roped together to give interpenetrated icosahedron segments, which give characteristic "fan"-like contrast under electron microscopy resembling that of half-spheres.[5b,c] Although our 2 nm Au−Ag NWs were very fragile under the electron beam in high-resolution TEM (HRTEM), we managed to capture quite a number of images where the “fan”-like contrast was a recurring feature (Figure 4).[8] These ordered patterns provide strong support against the possibility of random polycrystalline structure in the NWs. On the basis of their close resemblance to the “fan”-like contrast observed and simulated by José-Yacamán’s team, it is likely that our Au−Ag NWs also have twisted lattice consisting of BCB type spirals. Though our NWs were much longer (5 μm vs 50 nm), the same chirality was maintained over an entire NW as indicated by the chirality in the resulting double helices (Figure 2g). Jointed segments with opposite chirality are expected to give non-helical section near the junction; this was not observed in the nicely wound double helices (e.g., the (Au−Ag)@Pd ones).

Icosahedron and the BCB-type lattice are made of tetrahedral units,[5b] which cannot closely pack with each other. For example, when five tetrahedra stack to form a decahedron, there is a misfit angle of 7.35°. The larger diameter of the Au−Ag NW is, the greater its lattice strain. Thus, upon metal deposition, the expansion of the NW lateral dimension increases the strain therein. In minimizing the overall lattice energy, the NWs were forced to untwist (twisting in the opposite direction of the BCB lattice). While the open ends of a NW can twist without intertwining, the high aspect ratio (>1000) makes it impossible to untwist the entire NW strictly along a same axis. Thus, the NW winds around itself to form a double helix, in much the same way an electric cord winds around itself upon twisting. Multiple bending sites in a long NW thus give multiple U-turn ends. The pitch length of BCB type spirals (3.7 nm) is much shorter than that of the (Au−Ag)@Pd double helices (47 nm). Hence, the excess twisting potential winds the double helix tightly together, leading to a constant pitch length. When Ag was partially removed from the Au−Ag NWs (Figure 3a), the reorganized lattice was directly compromised without untwisting (Figure 3b).

In summary, we report the winding of ultrathin NWs to form double helices. The chemistry of the NWs provides rich information for mechanistic inference. Their chiral action is a dramatic display of the chirality at atomic scale. The predictable motion of nanostructure upon chemical stimuli could be potentially exploited for developing smart nanodevices.

■ ASSOCIATED CONTENT

Ⓢ Supporting Information. Details for experimental procedures, large-area views of TEM images. This material is available free of charge via the Internet at http://pubs.acs.org.

■ AUTHOR INFORMATION

Corresponding Author

hongyuchen@ntu.edu.sg

■ ACKNOWLEDGMENT

We thank Prof. Chan Yin Thai from National University of Singapore for the helpful advice. This work was supported by the MOE (ARC 13/09) and A*Star (102-152-0018) of Singapore.

■ REFERENCES

(1) (a) Thomas, J. M.; Raja, R. *Acc. Chem. Res.* **2008**, *41*, 708. (b) Hazen, R. M.; Sholl, D. S. *Nat. Mater.* **2003**, *2*, 367. (c) Shemer, G.; Krichevski, O.; Markovich, G.; Molotsky, T.; Lubitz, I.; Kotlyar, A. B. *J. Am. Chem. Soc.* **2006**, *128*, 11006. (d) Chen, W.; Bian, A.; Agarwal, A.; Liu, L. Q.; Shen, H. B.; Wang, L. B.; Xu, C. L.; Kotov, N. A. *Nano Lett.* **2009**, *9*, 2153. (e) Oh, H. S.; Liu, S.; Jee, H.; Baev, A.; Swihart, M. T.; Prasad, P. N. *J. Am. Chem. Soc.* **2010**, *132*, 17346. (f) Li, C.; Deng, K.; Tang, Z. Y.; Jiang, L. *J. Am. Chem. Soc.* **2010**, *132*, 8202.

(2) Perro, A.; Reculusa, S.; Ravaine, S.; Bourgeat-Lami, E. B.; Duguet, E. *J. Mater. Chem.* **2005**, *15*, 3745.

(3) (a) Amelinckx, S.; Zhang, X. B.; Bernaerts, D.; Zhang, X. F.; Ivanov, V.; Nagy, J. B. *Science* **1994**, *265*, 635. (b) Gao, P. X.; Ding, Y.; Mai, W.; Hughes, W. L.; Lao, C.; Wang, Z. L. *Science* **2005**, *309*, 1700. (c) Wang, H. T.; Wu, J. C.; Shen, Y. Q.; Li, G. P.; Zhang, Z.; Xing, G. Z.; Guo, D. L.; Wang, D. D.; Dong, Z. L.; Wu, T. *J. Am. Chem. Soc.* **2010**, *132*, 15875.

(4) (a) Wu, Y. Y.; Cheng, G. S.; Katsov, K.; Sides, S. W.; Wang, J. F.; Tang, J.; Fredrickson, G. H.; Moskovits, M.; Stucky, G. D. *Nat. Mater.* **2004**, *3*, 816. (b) Xu, J.; Wang, H.; Liu, C. C.; Yang, Y. M.; Chen, T.; Wang, Y. W.; Wang, F.; Liu, X. G.; Xing, B. G.; Chen, H. Y. *J. Am. Chem. Soc.* **2010**, *132*, 11920. (c) Chen, L. Y.; Wang, H.; Xu, J.; Shen, X. S.; Yao, L.; Zhu, L. F.; Zeng, Z. Y.; Zhang, H.; Chen, H. Y. *J. Am. Chem. Soc.* **2011**, *133*, 9654. (d) Liu, L. C.; Yoo, S. H.; Lee, S. A.; Park, S. *Nano Lett.* **2011**, *11*, 3979.

(5) (a) Kondo, Y.; Takayanagi, K. *Science* **2000**, *289*, 606. (b) Velázquez-Salazar, J. J.; Esparza, R.; Mejía-Rosales, S. J.; Estrada-Salas, R.; Ponce, A.; Deepak, F. L.; Castro-Guerrero, C.; José-Yacamán, M. *ACS Nano* **2011**, *5*, 6272. (c) Ascencio, J. A.; Gutiérrez-Wing, C.; Espinosa, M. E.; Marín, M.; Tehuacanero, S.; Zorrilla, C.; José-Yacamán, M. *Surf. Sci.* **1998**, *396*, 349.

(6) (a) Rycenga, M.; Cobley, C. M.; Zeng, J.; Li, W. Y.; Moran, C. H.; Zhang, Q.; Qin, D.; Xia, Y. N. *Chem. Rev.* **2011**, *111*, 3669. (b) Millstone, J. E.; Hurst, S. J.; Metraux, G. S.; Cutler, J. I.; Mirkin, C. A. *Small* **2009**, *5*, 646.

(7) (a) Xing, S. X.; Tan, L. H.; Chen, T.; Yang, Y. H.; Chen, H. Y. *Chem. Commun.* **2009**, 1653. (b) Xing, S. X.; Feng, Y. H.; Tay, Y. Y.; Chen, T.; Xu, J.; Pan, M.; He, J. T.; Hng, H. H.; Yan, Q. Y.; Chen, H. Y. *J. Am. Chem. Soc.* **2010**, *132*, 9537. (c) Pan, M.; Xing, S. X.; Sun, T.; Zhou, W. W.; Sindoro, M.; Teo, H. H.; Yan, Q. Y.; Chen, H. Y. *Chem. Commun.* **2010**, *46*, 7112. (d) Xing, S. X.; Tan, L. H.; Yang, M. X.; Pan, M.; Lv, Y. B.; Tang, Q. H.; Yang, Y. H.; Chen, H. Y. *J. Mater. Chem.* **2009**, *19*, 3286.

(8) See Supporting Information for details and large-view images.

(9) (a) Wang, C.; Sun, S. H. *Chem.—Asian J.* **2009**, *4*, 1028. (b) Hong, X.; Wang, D. S.; Yu, R.; Yan, H.; Sun, Y.; He, L.; Niu, Z. Q.; Peng, Q.; Li, Y. D. *Chem. Commun.* **2011**, *47*, 5160. (c) Feng, H. J.; Yang, Y. M.; You, Y. M.; Li, G. P.; Guo, J.; Yu, T.; Shen, Z. X.; Wu, T.; Xing, B. G. *Chem. Commun.* **2009**, 1984.

(10) (a) Krichevski, O.; Tirosh, E.; Markovich, G. *Langmuir* **2006**, *22*, 867. (b) He, J. T.; Wang, Y. W.; Feng, Y. H.; Qi, X. Y.; Zeng, Z. Y.; Teo, W. S.; Zhang, H.; Chen, H. Y. 2011, in preparation.

(11) Lu, X. M.; Yavuz, M. S.; Tuan, H. Y.; Korgel, B. A.; Xia, Y. N. *J. Am. Chem. Soc.* **2008**, *130*, 8900.

(12) Teng, X. W.; Wang, Q.; Liu, P.; Han, W.; Frenkel, A.; Wen, W.; Marinkovic, N.; Hanson, J. C.; Rodriguez, J. A. *J. Am. Chem. Soc.* **2008**, *130*, 1093.

(13) Fan, F. R.; Liu, D. Y.; Wu, Y. F.; Duan, S.; Xie, Z. X.; Jiang, Z. Y.; Tian, Z. Q. *J. Am. Chem. Soc.* **2008**, *130*, 6949.

(14) Teng, X. W.; Han, W. Q.; Ku, W.; Hucker, M. *Angew. Chem., Int. Ed.* **2008**, *47*, 2055.